Self-organized nanoscale multilayer growth in hyperthermal ion deposition

I. Gerhards,* H. Stillrich, C. Ronning, and H. Hofsäss
2nd Institute of Physics, University of Göttingen, Friedrich-Hund-Platz 1, 37077 Göttingen, Germany

M. Seibt
4th Institute of Physics, University of Göttingen, Friedrich-Hund-Platz 1, 37077 Göttingen, Germany
(Received 2 April 2004; revised manuscript received 19 August 2004; published 15 December 2004)

In the course of thin film growth by co-deposition of low energy mass selected carbon and metal (Au or Fe) ions, an effect of self-organization was found. Although carbon and metal ions were deposited quasi-simultaneously, a multilayer film structure of alternately metal-rich and metal-deficient layers was grown. The period of these layers is of the order of a few nanometers (~6-20 nm), and the metal-rich layers consist of metallic nanocrystals. The multilayer formation process is discussed in comparison with earlier studies on C-Cu and C-Ag films with respect to the structural properties of small clusters of the different metals, the influence of sputtering yields, and the deposition parameters. For a variety of compound thin film materials we expect a multilayer structure to develop during simultaneous sputter deposition or ion beam deposition of the components. The suppositions for this scenario are: (a) the deposited elements are immiscible or there are immiscible phases of a compound material, (b) the sputtering yields of the film components imposed by the impinging species are in an appropriate range, and (c) one compound segregates at the surface.

DOI: 10.1103/PhysRevB.70.245418 PACS number(s): 61.46.+w, 79.20.Rf

I. INTRODUCTION

Nanostructured materials, especially those that can be synthesized into any kind of ordered structure in a controlled manner, are currently of great interest. These materials are expected to constitute the principal component of most future electronic devices. In order to develop production techniques of industrial interest, a thorough understanding of the mechanisms governing the growth of different nanostructures is essential. Of course, the number of different methods of synthesis in thin film processing is very large, and the mechanisms differ greatly. The deposition of hyperthermal species, i.e., species with energies of >1 eV, is an athermal process and leads to a subsurface growth of thin films. It can be used to synthesize materials such as tetrahedrally bonded amorphous carbon,[1] cubic boron nitride thin films,[2] or even nucleate diamond.[3] Hyperthermal deposition techniques comprise methods such as ion beam assisted deposition[4] or deposition of low energy ions.[5] Among all hyperthermal species deposition techniques, the mass selective ion beam deposition is especially suitable for exploring growth mechanisms as the deposition parameters can be chosen independently and only the selected species (e.g., singly charged ions) contribute to the film growth.

Self-organization effects have been reported on scales of almost any order of magnitude.[6] They are of considerable value for the generation of low-dimensional semiconductor structures, as lithography and etching-based fabrication are complicated processes. A number of examples is given by Moriarty:[7] Semiconductor nanoclusters with narrow size distributions grow self-assembled on semiconductor substrates due to a lattice mismatch of the cluster and substrate materials. Also, lateral positioning of clusters can be controlled by using a suitably prepared substrate. A formation of a multilayer film structure with layer periods in the order of nanometers is known, for instance, from layer-by-layer self-assembly[8] or Liesegang patterns.[9] The layer-by-layer self-assembly process relies on the self-assembled adsorption from alternately polyanionic or polycathionic aqueous solutions onto a substrate. Liesegang patterns, which can be created by implanting specific impurities into a material, are experimentally closer to our work. The impurity concentration profile is approximately a Gaussian distribution centered at the mean ion range given by the implantation energy. Under thermal treatment, the concentration gradients lead to diffusion. Successional crystallization of a certain phase at a specific concentration then results in a multilayer film structure. The thermodynamic effect behind many cases of self-organization is the spinodal decomposition.[10] In the case of supercooling, an alloy is unstable against concentration fluctuations when the second derivative of the molar free energy with respect to the concentration of one component is negative. This results in a negative interdiffusion coefficient.

Recently, Wu and Ting found a self-organized formation of alternately metal-rich and metal-deficient multilayers of carbon-metal films gown by sputtering deposition.[11] The energies of the species deposited by sputtering techniques are explicitly smaller than for hyperthermal ion deposition. Wu and Ting explain the multilayer formation taking surface effects and deposition rates as well as the catalytic behavior of metals into account.

In this paper, we report on an effect of self-organization in the course of co-deposition of carbon and metal ions into multilayer thin films. Such a film morphology is found for composites of carbon and gold as well as carbon and iron. The samples discussed in this study were not thermally treated or subjected to heating during the deposition process. Furthermore, they do not resemble a supercooled liquid at any stage of the deposition process. The formation mechanisms will be discussed, taking into account the results from previous studies on films grown by co-deposition of carbon and either copper or silver ions.[12,13] While the carbon-copper

films consisted of nm-sized copper clusters embedded in an amorphous carbon matrix, the silver fully segregated at the surface of the films and was either sputtered away in the deposition process or accumulated to form clusters at the surface. In order to explain the morphologies of the different composites, the properties of small clusters of each metal will be considered. The formation of a multilayer structure will be explained in a model considering basic ion-solid interaction processes, such as sputtering and ion beam induced atomic rearrangements within the film.

II. EXPERIMENT

Carbon-metal composite thin films were grown by mass selective ion beam deposition (MSIBD). This unique method allows a very clean film growth with well definable deposition parameters; only the selected ions with the given kinetic energy contribute to the film growth.[14] We used $^{12}C^+$ and $^{197}Au^+$ or $^{56}Fe^+$ ions, respectively, for the co-deposition of thin films onto silicon substrates. Au is noncarbide forming and immiscible with carbon.[15] The carbide forming metal Fe was chosen for comparison. All samples were grown at room temperature and pressures of $\leqslant 10^{-6}$ mbar. In order to grow the C-Au films, $^{197}Au^+$ and $^{12}C^+$ ions were produced in a Penning sputter ion source with an extraction voltage of 22 kV. While a Penning sputter ion source allows one to produce an Au ion beam current large enough for film deposition, it also has the disadvantage of a rather broad ion energy distribution ($\sim$40 eV under the present source parameters). A hot filament hollow cathode ion source with a much better energy resolution was used to produce $^{56}Fe^+$ ions, and the extraction voltage was 30 kV. Isotopically pure ion beams of $^{12}C^+$ and an isotope of the particular metal were alternately selected by a sector magnet and focused into the deposition chamber by an ion optical setup. The beam was scanned over the substrate by a beam sweep in order to ensure a laterally uniform film growth. Before impinging on the substrate, the ions were decelerated to the desired kinetic energy. The deposited ion charge derived from the time-integrated measurement of the ion current on the substrate was used to rapidly switch the separation magnet between the different ion species in order to grow composite films with a predefined composition. A fluence of at most 10^{15} ions/cm^2 per switching cycle was divided into the desired carbon-metal fluence ratio $r_{fluence}=f_C/f_M$, where f_C and f_M are the carbon and metal fluence fractions, respectively. By repeating these cycles about 1000 times, films of typically about 50 nm thickness were grown. The implantation profiles at these values overlap almost perfectly and deposition in this manner resembles the simultaneous deposition of both ion species. In this way, homogeneous film growth has been achieved for various binary compounds, such as cubic boron nitride, boron carbide, or carbon nitride.[16–18] A uniform distribution of nm-size Cu crystals embedded in an amorphous carbon matrix was also grown in the same manner.[12,13] A more detailed description of the experimental setup and theoretical treatment of the deposition process can be found elsewhere.[17,19] For each of the carbon-metal composite thin film systems, a set of samples was deposited with different carbon-metal fluence ratios $r_{fluence}$. The deposition parameters are listed in Table I.

TABLE I. Overview of the deposition parameters. All samples were deposited at room temperature onto *p*-Si (100) substrates.

	$r_{fluence}$	C^+ ion energy [eV]	Metal$^+$ ion energy [eV]	Total film thicknesses (nm)
C-Au	4–19	100–150	100–150	40–60
C-Fe	1–19	100	40	25–30

The carbon ion energy was chosen to be about 100 eV, where the maximum sp^3 bonding content is to be expected.[20] The metal ion energy should be selected at a lower value (i.e., 40 eV for the C-Fe films) in order to avoid severe sputtering. For the C-Au films, however, the ion energies could not be chosen independently for both ion species, and smaller energies are difficult to achieve due to the properties of the experimental setup. Under the given conditions, ions are implanted about 1–3 nm below the substrate surface. This is a process far from thermodynamic equilibrium and often described as subplantation or deposition of hyperthermal species.[21,22]

The films were analyzed by Rutherford backscattering spectroscopy (RBS) in order to determine the integral film composition and obtain a depth profile of the metal atom concentration. RBS was performed at the Göttingen heavy ion implanter IONAS,[23] using 900 keV He^{2+} ions. For this ion energy, the electronic stopping power reaches its maximum and therefore provides a high depth resolution of $\leqslant$10 nm. The He^{2+} ion beam was aimed at each sample perpendicular to the sample surface, and the detector was placed at an angle of 168.5° with respect to the incident ion beam direction. The RBS data were analyzed using the RUMP and NDF software packages.[24,25] High resolution transmission electron microscopy (HRTEM) and energy dispersive x-ray spectroscopy (EDX) were conducted on a Philips CM 200–UT equipped with a field emission electron source. The scanning mode of the microscope allows the measurement of EDX line scans along a defined path. This makes it very convenient for a qualitative depth-resolved analysis of the metal concentration of the thin film structures. One C-Au sample with a sufficient amount of Au was analyzed by x-ray diffraction on a Bruker AXS D8 x-ray diffractometer equipped with a Cu anode. The x-ray wavelength applied was 0.154 nm.

Sputtering is one of the major factors influencing the film growth by ion beam deposition. We used SRIM[26] calculations to estimate the sputtering yields of Au by Au and C ions (see Table II). Comparison of these sputtering yields with the RBS composition analyses gives insight into the growth mechanisms, as sputtering is a surface effect. Table II also includes SRIM sputtering yields of Cu and Ag. These are necessary for comparison.

III. RESULTS

In the following we present the results of transmission electron microscopy (TEM), EDX and RBS analyses on the C-Au and C-Fe films.

TABLE II. SRIM calculated self-sputtering yields s_{MM} (M=Cu, Ag, Au) and sputtering yields s_{CM} of metal atoms by incident carbon ions of the respective energies.

Ion impinging on Cu	s_{CuCu} s_{CCu}	Ion impinging on Ag	s_{AgAg} s_{CAg}	Ion impinging on Au	s_{AuAu} s_{CAu}
40 eV Cu^+	0.10	60 eV Ag^+	0.18	100±30 eV Au^+	0.37
80 eV C^+	0.22	80 eV C^+	0.04	100±30 eV C^+	0.03

A. Carbon-gold films

Figure 1 depicts an overview transmission electron micrograph of the entire cross section of a C-Au sample deposited with a carbon-gold fluence ratio of $r_{fluence}=4$. A multilayer structure is clearly distinguishable in the overview micrograph with layer distances between 3 and 15 nm. The first dark layer following the interface to the Si substrate is a mixture of C, Au, and Si atoms formed at the beginning of the deposition process when the first incoming ions were subplanted into the topmost nanometers of the Si substrate. The successive layers are alternately Au-deficient and Au-rich. The layer structure was verified by EDX line scans across the film (not shown). The sectors indicated in the overview micrograph were analyzed in high resolution mode (see insets of Fig. 1). These micrographs reveal a nanocrystalline structure in the Au-rich layers and an amorphous structure in the Au-deficient regions. Fourier transformations of the micrographs of the crystalline particles match the {111} lattice plane spacing of Au of 0.24 nm. An x-ray diffractogram of this sample shows several Au signals. Using the Scherrer formula,[27] an approximate average cluster diameter of 5 nm from the linewidth of the Au (111) signal can be derived. Figure 2 shows the RBS spectrum of the sample shown in the TEM micrograph of Fig. 1. The Au signal exhibits a double peak structure, which indicates an inhomogeneous Au concentration depth profile. Using the information gained from TEM for a RUMP analysis of the appendant RBS spectrum, one obtains the simulated plot depicted in Fig. 2. The inset of Fig. 2 accounts for the assumed layer composition for the RUMP simulation. The first two gold-rich layers give rise to the higher energy peak of the spectrum, the lower energy peak is dominated by the third gold-rich layer and the mixture layer leads to a slight shoulder to the lower energy side of the signal. However, as the layer periods partly fall below the depth resolution of the RBS setup, the results should not be over interpreted. The integral film composition determined from the RBS spectra of all samples reveals that there is a significant shortage of Au compared to the deposited Au ion fluence. About 50% of the deposited Au atoms are sputtered off the film.

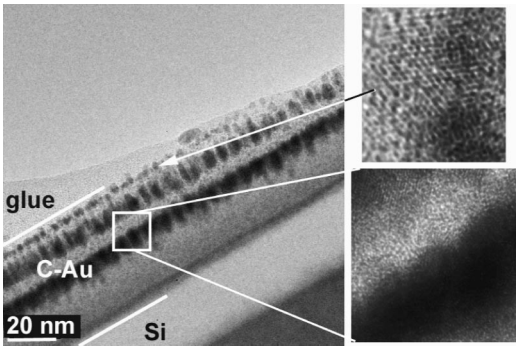

FIG. 1. TEM micrographs of a self-organized C-Au multilayer film deposited with a carbon-gold fluence ratio of $r_{fluence}=4$. The layer structure is clearly visible. The augmentations show crystalline particles in the darker layers and an amorphous structure of the brighter layers.

B. Carbon-iron films

Although the C-Fe system is very different from the C-Au system, these films show similar layer structures. Figure 3 shows a TEM micrograph of a sample deposited with a carbon-iron fluence ratio $r_{fluence}=4$. The dark layer at the substrate interface is a Si-C-Fe mixture phase similar to the Si-C-metal mixture phases described above for the C-Au films. EDX confirms that the subsequent brighter layers seen in Fig. 3 are deficient in iron compared to the iron-rich darker layers. From TEM and the EDX line scan we can derive the period of the iron-rich layers to about 6–7 nm. The Fe areal densities of the films measured by RBS resemble the deposited iron ion fluences (see Fig. 4). As obviously no sputtering of Fe atoms off the film surface occurs, we deduce that the surface consists of only C atoms during the entire deposition process. Therefore, the interface indicated in Fig. 3. between the sample surface and the glue used

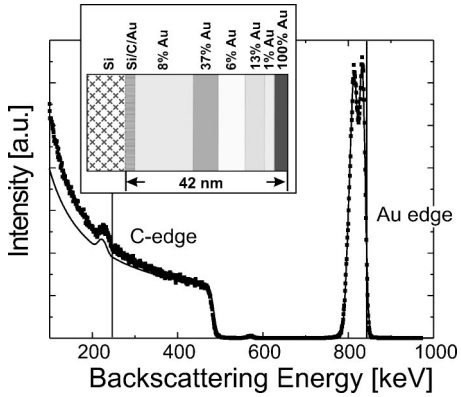

FIG. 2. RBS spectrum of a sample deposited with a carbon-gold fluence ratio of $r_{fluence}=4$. The Au signal exhibits a double peak structure that indicates a multilayer morphology of the film. The inset shows the layer sequence that was assumed for the simulation of the spectrum. The layer thicknesses, starting from the surface, are 3.5, 2.5, 5, 7, 6.5, and 15 nm. The mixture layer has a thickness of 2.5 nm.

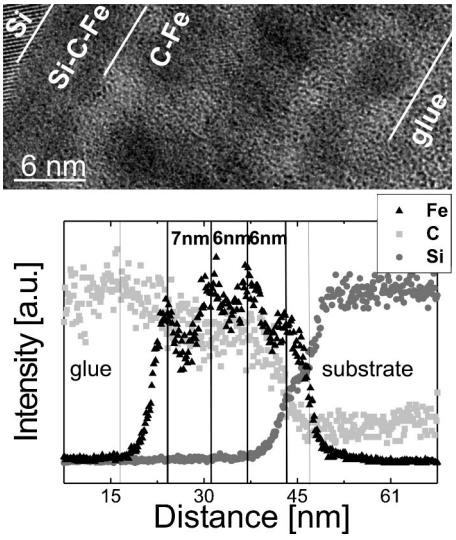

FIG. 3. (Top) HRTEM micrograph of the C-Fe film containing 20% Fe. The darker stripes contain a larger number of crystalline iron carbide clusters, whereas the brighter areas consist of amorphous carbon. (Bottom) EDX line scan of the same film. The iron signal varies periodically over the whole depth of the film, clearly exhibiting 4 maxima with distances of 6–7 nm. The maxima of the Fe signal correspond to the darker layers in the micrograph.

for preparation can only be estimated: the glue cannot be distinguished from the amorphous carbon in the micrograph and the carbon signal in the EDX line scan shows no notable change, as the glue also contains a significant amount of carbon.

Not all of the RBS spectra measured for the C-Fe films show a double peak structure of the metal signal as is the case for the C-Au films. A double peak Fe signal is only observed in the RBS spectrum of the film of the lowest Fe concentration of 5%. For higher Fe contents, the distances between the layers are too narrow to be resolved by RBS.

IV. DISCUSSION

First, we exclude that the formation of the multilayers is an experimental artifact. The results of the TEM and RBS depth profile analyses are in good agreement. Therefore, we can eliminate the possibility of TEM sample preparation artifacts. Furthermore, the number of layers in the multilayer films (e.g., the sample depicted in the micrograph in Fig. 2) is about three orders of magnitude smaller than the number of switching cycles during deposition, and the deposited fluence for each cycle is far too small to account for the layer thicknesses. The multilayer structure is therefore not a result of a rapid sequential deposition process but a form of self-organization.

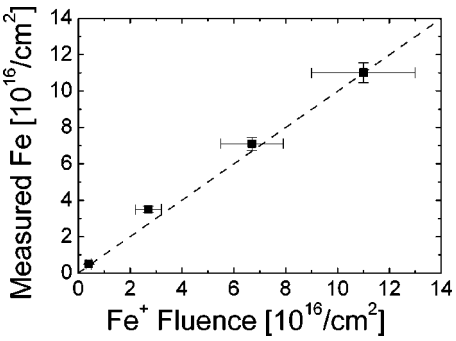

FIG. 4. The iron areal atomic density of the films is given in dependence of the deposited iron ion fluence. All iron atoms are fully incorporated into the films. Apparently, iron is not subject to sputtering.

In order to understand the structure formation during ion beam deposition, we have to take into account an atomic transport mechanism inside the film, which can either be thermally activated or ion induced. All the samples were grown at room temperature. The ion current densities were low ($<15\ \mu A/cm^2$) and did not cause any global heating of the sample. Previous studies by Kröger *et al.*[28] showed no diffusion of Cu and Ag and several other elements upon thermal treatment up to 1000 °C within diamond-like amorphous carbon environments. Thus, we exclude thermally activated diffusion of atoms within the films and Ostwald ripening, a basic process leading to cluster formation. Instead, we consider ion induced transport processes as described in the following: according to various models describing the film growth with ion beam deposition techniques, an incoming ion severely changes the atomic structure of the close environment of its path (subplantation models by Lifshitz and Robertson,[21,22,29,30] stress models by Davis and McKenzie,[31–33] cylindrical thermal spike model by Hofsäss.[19]) For the ion energies chosen in the experiment, these models suggest significant atomic rearrangements along the length of the ion path $r_I(\sim 1-3$ nm) during a time scale of about 10^{-12} s, before the impact energy is dissipated. The cylindrical thermal spike model predicts typically 10–20 rearranged atoms per ion impact. The processes involved are far from thermodynamic equilibrium and the material does not resemble a supercooled liquid at any stage of the deposition process. A description on the basis of spinodal decomposition is therefore not applicable. Furthermore, spinodal decomposition would not be able to account for the formation of a multilayer structure in the C-Au and C-Fe case on the one hand and a homogeneous cluster formation, as it was found for C-Cu films[13] on the other hand.

Let us consider a random walk diffusion of metal atoms, where each diffusion step is triggered by a single ion impact. A given metal atom in the collision cascade volume is rearranged approximately once for each ion impact process,[19] and we assume that it travels a distance of one typical atom spacing a (≈ 0.15 nm for amorphous carbon). Once the film thickness has increased by the mean ion range r_I, we estimate that successive ion impacts have resulted in $N \approx 10^2-10^3$ rearrangement steps of a particular atom. If we assume a uniform three-dimensional random walk diffusion,[34] the average traveled distance $\overline{x}=\sqrt{3Na^2}$ results in 2–5 nm. This is sufficient to account for the cluster formation within an amorphous carbon matrix as well as the transport of atoms to the film surface if the diffusion direction is preferentially oriented.

TABLE III. Total sputtering yield induced by both carbon and metal ions. The values $S_M^{SRIM} = r_{fluence} s_{CM} + s_{MM}$ were calculated using the sputtering yields given in Table II. The S_M^{RBS} values were determined from RBS measurements. In the C-Cu case, these have to be compared with the values of $c_{surf} S_M^{SRIM}$, as the sample surface contains only a fraction $c_{surf} = f_M = f_C / r_{fluence}$ of Cu atoms.

	Cu			Ag		Au	
$r_{fluence}$	S_M^{SRIM}	S_M^{RBS}	$c_{surf} S_M^{SRIM}$	S_M^{SRIM}	S_M^{RBS}	S_M^{SRIM}	S_M^{RBS}
19				0.94	0.90±0.04	0.94	0.50±0.3
9	2.08	0.38±0.10	0.21	0.54	0.95±0.04	0.64	
4	0.98	0.26±0.11	0.20	0.34	0.69±0.04	0.49	0.50±0.3
2.33	0.61	0.12±0.14	0.18	0.27	0.44±0.04		
1.5	0.43	0.20±0.13	0.17				
1	0.32	0.10±0.14	0.16				

A. Three cases of structure formation

We will now describe the multilayer formation for the immiscible case of C and Au and the case of the carbide forming metal Fe in comparison with the formation of a uniform cluster distribution found for C-Cu films and a complete surface segregation of Ag in the case of co-deposition of C and Ag ions. We will consider ion-solid interaction processes along with the properties of small clusters of the respective metal:

(i) The case of uniform cluster distribution: carbon-copper films depostited using MSIBD consist of nm-sized copper clusters distributed uniformly within an amorphous carbon matrix.[13] The mean cluster diameter is tunable between about 3.5 and 9 nm by selecting different ion fluence ratios $r_{fluence} = 19 \ldots 1$.

As described above, we assume that a copper atom within the film moves one typical atom spacing into a random direction with each ion impact in its immediate neighborhood. When it meets another Cu atom, a dimer will be formed. This dimer (or a cluster of a small number of atoms that is formed in a subsequent process) is assumed to be stable under further ion impacts. Since copper is immiscible with carbon, the formation of precipitates is energetically favorable.

This scenario is supported by studies on the stability of small copper clusters: in an experiment by Chey, Huang, and Weaver,[35] Cu clusters were attempted to be moved across Si(111)-(7×7) surfaces using the tip of a scanning tunneling microscope (STM). The Cu clusters could not be moved and broke, when the applied force was too strong. A theoretical examination shows that small Cu clusters have geometrical structures with icosahedral packing[36] and are rather rigid. We can therefore assume Cu clusters to be stable against ion impact at the regarded energies. The clusters can grow as newly deposited Cu atoms encounter them in their ion impact triggered random walk. A rather homogeneous cluster distribution within the amorphous carbon matrix arises. The mean cluster size is related to the average metal concentration and the mean traveled path $\overline{x}$ of Cu atoms. The cluster diameters are expected to be a few nm, which is confirmed by TEM of C-Cu films.

Under steady-state conditions, the sputtering yield for metal atoms per incoming metal ion is given by

$$S_M = r_{fluence} s_{CM} + s_{MM}, \quad (1)$$

where s_{CM} and s_{MM} are the sputtering yields of metal atoms due to impinging carbon ions and the respective metal ions if a metal surface is assumed. The sputtering loss of metal atoms, however, also depends on the respective average surface concentration c_{surf}, which should be proportional to the metal ion fraction f_M in the case of isotropic ion triggered diffusion. From the RBS analysis of the C-Cu samples,[13] we find an average sputtering loss of $\overline{S_M} = 0.21 \pm 0.05$. A dependence on the metal ion fraction f_M cannot be claimed from the RBS results, as the errors are too large. However, the experimental values are in accordance with the calculated values $c_{surf} S_M^{SRIM}$, as shown in Table III.

(ii) The case of metal surface segregation: in preliminary studies we found that the co-deposition of C^+ and Ag^+ ions, similar to the way described above, resulted in a complete segregation of the Ag atoms at the surface, where they either formed clusters or were nearly completely sputtered off the film.[12] We therefore assume that small Ag clusters that may have formed in the ion impact triggered diffusion process do not resist successive ion impacts and the Ag atoms are dispersed. This assumption is in agreement with the abovementioned experiment by Chey, Huang, and Weaver.[35] The attempt to move Ag clusters across the Si(111)-(7×7) surfaces with the STM tip was successful and resulted in a track of Ag atoms along the path the cluster was moved (an effect described as *nanopainting*). Furthermore, a theoretical analysis shows that Ag clusters can be well described by an ellipsoidal jellium model that neglects the geometrical structure[37] and can be regarded as liquid droplets in contrast to the rigid Cu clusters.

The Ag atoms are eventually transported towards the surface. The driving forces behind the surface segregation are most likely the density gradient and the compressive stress that is characteristic for ion beam deposited films. We assume that this scenario also applies to the case of the C-Au films, as small Au clusters can also be described by a liquid drop model.[38]

The Ag or Au atoms that reach the sample surface in the course of ion impact induced diffusion are then subjected to severe sputtering.[31–35] This is in agreement with the results from the RBS analysis, which in this case have to be com-

pared directly to the values calculated from Eq. (1), because almost all metal atoms segregate at the film surface and are therefore subjected to sputtering. For both, C-Ag and C-Au films, RBS analysis reveals larger sputtering losses of metal atoms than for the C-Cu films. The measured sputtering losses vary between 0.44 ± 0.04 and 0.9 ± 0.04 for Ag and are about 0.5 ± 0.03 for Au.

Considering a given metal that segregates at the surface, there are two possible cases: either the sputtering yield S_M given by Eq. (1) is greater than 1. Then, all metal atoms are sputtered off the film. Or the sputtering yield depending on the ion fluence ratio and the ion energies is $S_M<1$. This results in an accumulation of metal atoms at the surface, as the supply of metal atoms by the incident ion beam exceeds the sputtering losses. While the clusters grow on the film surface, incoming C^+ ions contribute to the growth of a carbon layer underneath. Eventually, spaces in between clusters are filled with carbon and the cluster layer is buried underneath a newly forming carbon layer. As long as the incoming metal ions reach the buried clusters when being subplanted into the film or during their rearrangement steps, they further contribute to the cluster growth of the buried layer. If not, they will again segregate at the newly forming carbon film surface. There, they form a new layer of metal clusters as incoming C^+ ions contribute to the growth of a metal-deficient layer separating the cluster layers. This applies in general to both the C-Au and C-Ag cases. The sputtering yield S_M is notably smaller than 1 for the C-Au samples that showed a multilayer structure. For the C-Ag samples, the sputtering yield S_M is close to 1 and it requires a very high fluence to form a surface cluster layer. Thus, we find only the beginning of a multilayer structure formation, i.e., Ag clusters on top of an amorphous carbon film.

(iii) The case of carbon surface segregation: this case applies to the C-Fe films. Iron carbides are rich in Fe (we assume the most frequent Fe_3C),[39] whereas the samples reported on in this article bear an average Fe content of 5%–20% at. Fe. Therefore, iron carbide clusters embedded in an amorphous carbon matrix will form. The deposited Fe ions accumulate in a buried iron carbide cluster layer until the Fe_3C stoichiometry is reached. The excess C atoms are transported out of the Fe_3C layers, most likely towards the surface, due to ion induced rearrangements. As a result, a pure carbon surface layer emerges. No Fe atoms are lost due to sputtering, because they are not transported to the surface in the deposition process. With increasing thickness of the amorphous carbon surface layer, the deposited Fe ions cannot reach the buried iron carbide cluster layer anymore, and a new iron carbide layer grows, separated from the previous one by a thin carbon-rich layer. As a result, a multilayer film structure evolves.

B. Estimation of the multilayer period

Now, we will estimate the period of the layer structures for the case of metal surface segregation, i.e., the C-Ag and C-Au films, based on sputter yield data and ion fluences. The films were deposited with a carbon-metal fluence ratio $r_{fluence}$. We apply the metal's bulk atomic density n_M and the bulk density of graphite n_C. The total sputtering yield S_M of the metal per incoming metal ion is extracted from RBS measurements and can, for comparison, be calculated from the SRIM data by Eq. (1). The sputtering yield of carbon by metal ions is zero for all conditions under investigation and the sputtering yield of carbon by carbon ions $s_{CC}\approx0.1$. The covering of the carbon layer with a layer of metal clusters may be incomplete, which is described by the covering factor c. The thickness d_M of the layer of metal clusters is taken from experimental data (TEM micrographs). The areal density N_M in this metal cluster layer is $N_M=n_M d_M c$. Using this, we calculate the necessary total metal fluence F_M that has to be deposited in order to grow one metal cluster layer and account for sputtering losses and the fraction of dispersed metal atoms that remain within the matrix, where f_{surf} gives the fraction of deposited metal atoms segregating at the surface

$$F_M=\frac{N_M}{(1-S_M)f_{surf}}=\frac{n_M d_M c}{(1-S_M)f_{surf}}. \tag{2}$$

The corresponding total fluence of carbon atoms is larger than F_M by a factor of the carbon-metal fluence ratio $r_{fluence}$

$$F_C=r_{fluence}F_M. \tag{3}$$

The deposition of this amount in addition to the fraction $(1-f_{surf})$ of dispersed metal atoms and lacking the amount of sputtered C atoms leads to a thickness d_C of the carbon layer of

$$d_C=\frac{F_C(1-s_{CC})}{n_C}+\frac{F_M(1-f_{surf})}{n_m}. \tag{4}$$

Applying Eqs. (2) and (3) to Eq. (4), the period $t=d_M+d_C$ results in

$$t=d_M\left[1+\frac{n_M c}{(1-S_M)f_{surf}}\times\left(\frac{1}{n_C}r_{f\ell fluence}(1-s_{CC})+\frac{1}{n_M}(1-f_{surf})\right)\right]. \tag{5}$$

This expression can be simplified if we assume a full segregation of the metal atoms at the surface, a complete coverage for the metal cluster layer, and negligible carbon sputtering ($f_{surf}=1$, $c=1$, $s_{CC}=0$)

$$t\approx d_M\left[1+\frac{n_M}{(1-S_M)}r_{fluence}\frac{1}{n_C}\right]. \tag{6}$$

Instead of a rectangular metal cluster layer with thickness d_M we should rather assume a layer with Gaussian concentration profile of the same areal density with a full width at half maximum (FWHM) value taken from the TEM and EDX analysis. Therefore, we have to replace $d_M=1.06\times\mathrm{FWHM}$ in Eqs. (5) and (6).

For the C-Au sample of Figs. 2 and 3, where $r_{fluence}=4$, $n_M=59/\mathrm{nm}^3$, and $n_C=110/\mathrm{nm}^3$, we derive $S_M=0.5$ and FWHM=5–9 nm from RBS and EDX analyses, and obtain a period of the layer structure using of $t\approx28$ nm, using Eq. (6). From the TEM micrographs and EDX analysis we find the experimental value $t_{exp}\approx14$ nm. It is, however, most

likely that the covering factor $c<1$. Although the TEM micrographs suggest complete layers of metal clusters, we presumably see clusters that are not in the interstice of two clusters but are rather behind this blank. A comparison of the Au areal density determined by RBS ($\approx 4\times 10^{16}$) with the necessary amount to create a multilayer structure with cluster layers of Au bulk density (1.6×10^{17}) results in a value of $c\approx 0.25$ to 0.3 and a layer period t, which is in good agreement with the experiment.

The period of the C-Fe multilayer structures can be estimated in analogy to the C-Au case, taking a few alterations into account. As the iron ions do not segregate at the film surface but accumulate in layers within the film, a parameter f_{layer}, which gives the fraction of iron atoms accumulating in an iron carbide cluster layer, has to be introduced. The fraction $1-f_{layer}$ of iron atoms is dispersed throughout the carbon-rich layers. Furthermore, we have to consider that the clusters of the metal-rich layers contain a significant amount of carbon which is not available for the separating carbon layers. If $n_{Fe_3C}=103/\mathrm{nm}^3$ is the atomic density of Fe_3C, the iron fluence for one cluster layer covered with a fraction c with clusters is

$$F_{\mathrm{Fe}}=\frac{0.75\cdot n_{\mathrm{Fe_3C}}\cdot d_M\cdot c}{f_{layer}}. \tag{7}$$

Of course, this again corresponds to a deposited carbon ion fluence of $F_C=r_{fluence}F_{\mathrm{Fe}}$. The thickness d_C of the carbon layer is reduced by the amount of carbon necessary to meet the Fe_3C stoichiometry and the sputtering of carbon atoms. It is, however, increased by the dispersed iron atoms, that do not add to the iron carbide cluster layers

$$d_C=F_{\mathrm{Fe}}\left(\frac{r_{fluence}(1-s_{CC})-0.25}{n_c}+\frac{1-f_{layer}}{n_{\mathrm{Fe}}}\right), \tag{8}$$

where $n_C=110/\mathrm{nm}^3$ and $n_{\mathrm{Fe}}=85/\mathrm{nm}^3$ are the atomic densities of graphite and iron, respectively. Applying Eq. (7) to Eq. (8), a period $t=d_M+d_C$ of

$$t=d_M\left[1+\frac{0.75\cdot n_{\mathrm{Fe_3C}}\cdot d_M\cdot c}{f_{layer}}\times\left(\frac{r_{fluence}(1-s_{CC})-0.25}{n_c}+\frac{1-f_{layer}}{n_{\mathrm{Fe}}}\right)\right] \tag{9}$$

results. Assuming a covering with metal clusters in each cluster layer of $c=0.7$ and that the fraction of iron atoms contributing to the cluster layers is $f_{layer}=0.7$, we get $t=7$ nm for the sample of Fig. 4, where $d_M\approx 2$ nm, $r_{fluence}=4$. This is again in good agreement with the results derived from TEM and EDX.

C. Predictions

From Eq. (5) it follows that the period of the layer structure strongly depends on the total sputtering yield of surface metal atoms $S_M=s_{MM}+r_{fluence}s_{CM}$. S_M itself depends on the ion energies and the carbon-metal fluence ratio $r_{fluence}$. A careful selection of these parameters allows the growth of multilayer structures with variable layer periods. If, however, $S_M>1$, all metal atoms are sputtered off the film and no layer structure can arise. The film contains only small amounts of dispersed metal atoms or small metal clusters, depending on f_{surf}. In order to grow metal clusters within a diamond-like amorphous carbon matrix, the carbon ion energy has to be kept at about 100 eV in order to achieve a high sp^3 bonding content. The energy of the metal ions should be raised so that the mean ion range well exceeds the carbon ion range of about 1 nm, and in addition $S_M>1$. The first condition increases the probability for metal atoms to remain within the amorphous carbon matrix and form clusters; the second one ensures that all surface metal atoms are completely sputtered off. The maximum metal ion energy is, however, limited to several hundred eV, because otherwise the sputtering yield of carbon by metal ions becomes significant. For the ion beam deposition of 1 keV Ag ions into tetrahedral amorphous carbon Kröger *et al.* observed that about 10% of the deposited Ag was incorporated in the film.[32]

For the case of carbon surface segregation, we derive from Eq. (9) that only a variation of the ion fluence ratio $r_{fluence}$ can influence the layer period.

V. CONCLUSION

We report an effect of self-organization in ion beam deposited C-Au and C-Fe films. The self-organized formation of metal-rich and metal-deficient multilayers during ion beam co-deposition of carbon and metal ions is attributed to an interplay between (a) the ion impact triggered atomic transport, (b) the segregation of metal atoms at the surface, (c) the preferential sputtering of surface metal atoms, and (d) the stability of small metal or metal carbide clusters under ion impact. Two extreme cases can be considered: first, when small metal clusters are stable under ion beam bombardment, their atoms do not participate in the ion impact triggered diffusion. Further incoming metal ions may add to the cluster. This way, the co-deposition of C and Cu ions results in a uniform cluster distribution and the cluster size is determined by the ion impact triggered diffusion of newly incoming metal ions towards an existing cluster and the carbon-metal fluence ratio. Second, if small metal clusters are unstable against ion irradiation, the metal atoms preferentially segregate at the surface. If the total sputtering yield due to impinging carbon and metal ions $S_M>1$, all surface metal atoms are sputtered off the film. If, however, $S_M<1$, metal atoms accumulate at the surface and larger clusters will be formed. Carbon ions that are deposited into the film, along with the metal ions, contribute to the growth of a carbon layer underneath the metal cluster layer, eventually fill spaces in between clusters, and bury the metal cluster layer. This leads to the formation of a multilayer structure as it was observed for the C-Au films. A complete decomposition into a carbon layer with a metal layer at its surface arises if the period under the given experimental conditions exceeds the film thickness. This is the case for the C-Ag films presented in this report. The layer period can be calculated using equation Eq. (6). This calculation substantiates the assumptions made

for the multilayer formation processes. However, the thickness of the metal layer was taken from TEM micrographs. It is, of course, desirable to be able to estimate this value from a certain knowledge of the materials properties, such as binding energies within small clusters, and the deposition parameters influencing the surface segregation the (ion enhanced) surface diffusion, and sputtering. The development of a complete model on the basis of a mean field nucleation theory as described by Brune[40] that would account for all parameters is, however, not easily established and would go beyond the scope of this study. A possible approach would be to extend a Monte Carlo program such as TRIDYN[41,42] in such a way that it covers the various processes involved in the formation of multilayers.

We expect the formation of a multilayer structure during co-deposition of two or more constituents to also occur for other composites and also for other techniques involving hyperthermal species. In particular, the formation of a multilayer structure is likely in the case of a low sputter yield S_M, as is the case for ion or plasma assisted sputter deposition.

ACKNOWLEDGMENTS

I. Gerhards and H. Hofsäss wish to thank H. Teichler for a discussion of the presented effect. I. Gerhards also expresses her gratitude to P. Reinke for stimulating discussions and remarks on the subject.

*Electronic address: igerhar@gwdg.de

[1] J. P. Zhao and Z. Y. Chen, Phys. Rev. B **63**, 115318 (2001).
[2] H. Hofsäss, H. Feldermann, S. Eyhusen, and C. Ronning, Phys. Rev. B **65**, 115410 (2002).
[3] Y. Lifshitz, Th. Köhler, Th. Frauenheim, I. Guzmann, A. Hoffman, R. Q. Zhang, X. T. Zhou, and S. T. Lee, Science **297**, 1531 (2002).
[4] J. W. Gerlach, R. Schwertberger, D. Schrupp, B. Rauschenbach, H. Neumann, and M. Zeuner, Surf. Coat. Technol. **128**, 286 (2000).
[5] B. Degroote, A. Vantomme, H. Pattyn, and K. Vanormelingen, Phys. Rev. B **65**, 195401 (2002).
[6] G. M. Whitesides and B. Grzybowski, Science **295**, 2418 (2002).
[7] P. Moriarty, Rep. Prog. Phys. **64**, 297 (2000), and references therein.
[8] G. Decher, Science **277**, 1232 (1997).
[9] R. E. Liesegang, Naturwiss. Wochenschr. **11**, 353 (1896).
[10] T. Antal, M. Droz, J. Magnin, and Z. Rácz, Phys. Rev. Lett. **83**, 2880 (1999).
[11] W.-Y. Wu and Y.-M. Ting, Chem. Phys. Lett. **388**, 312 (2004).
[12] I. Gerhards, C. Ronning, U. Vetter, H. Hofsäss, H. Gibhardt, G. Eckold, Q. Li, S. T. Lee, Y. L. Huang, and M. Seibt, Surf. Coat. Technol. **158–159**, 114 (2002).
[13] I. Gerhards, C. Ronning, H. Hofsäss, M. Seibt, and H. Gibhardt, J. Appl. Phys. **93**, 1203 (2003).
[14] H. Hofsäss, H. Binder, T. Klumpp, and E. Recknagel, Diamond Relat. Mater. **3**, 137 (1994).
[15] *Binary Alloy Phase Diagrams*, edited by T. B. Massalski, H. Okamoto, P. R. Subramanian, and L. Kacprzak (ASM, Metal Park, OH 1996).
[16] H. Hofsäss, C. Ronning, U. Griesmeier, M. Gross, S. Reinke, and M. Kuhr, Appl. Phys. Lett. **67**, 46 (1995).
[17] C. Ronning, D. Schwen, S. Eyhusen, U. Vetter, and H. Hofsäss, Surf. Coat. Technol. **158–159**, 382 (2002).
[18] C. Ronning, H. Feldermann, R. Merk, H. Hofsäss, P. Reinke, and J.-U. Thiele, Phys. Rev. B **58**, 2207 (1998).
[19] H. Hofsäss, H. Feldermann, R. Merk, M. Sebastian, and C. Ronning, Appl. Phys. A: Mater. Sci. Process. **66**, 153 (1998).
[20] C. Ronning, E. Dreher, J.-U. Thiele, P. Oelhafen, and H. Hofsäss, Diamond Relat. Mater. **6**, 830 (1997).
[21] Y. Lifshitz, S. R. Kasi, and J. W. Rabalais, Phys. Rev. Lett. **62**, 1290 (1989).
[22] Y. Lifshitz, S. R. Kasi, J. W. Rabalais, and W. Eckstein, Phys. Rev. B **41**, 10 468 (1990).
[23] M. Uhrmacher, K. Pampus, F. J. Bergmeister, D. Purschke, and K. P. Lieb, Nucl. Instrum. Methods Phys. Res. B **9**, 234 (1985).
[24] L. R. Doolittle, Nucl. Instrum. Methods Phys. Res. B **15**, 227 (1986).
[25] N. P. Barradas, C. Jeynes, and R. P. Wepp, Appl. Phys. Lett. **71**, 291 (1997).
[26] J. F. Ziegler, J. P. Biersack, and U. Littmark, *The Stopping and Range of Ions in Solids* (Pergamon, New York, 1985). Free download: http://srim.org
[27] B. D. Cullity and S. R. Stock, *Elements of X-ray Diffraction* (Prentice Hall, Englewood Cliffs, NJ, 2001).
[28] H. Kröger, C. Ronning, H. Hofsäss, P. Neumaier, A. Bergmaier, L. Görgens, and G. Dollinger, Diamond Relat. Mater. **12**, 2042 (2003).
[29] J. Robertson, Diamond Relat. Mater. **2**, 984 (1993).
[30] J. Robertson, Diamond Relat. Mater. **3**, 361 (1994).
[31] C. A. Davis, Thin Solid Films **226**, 30 (1993).
[32] D. R. McKenzie, D. Muller, B. A. Pailthorpe, Z. H. Wang, E. Kravtchinskaia, D. Segal, P. B. Lukins, P. D. Swift, P. J. Martin, G. Amaratunga, P. H. Gaskell, and A. Saeed, Diamond Relat. Mater. **1**, 51 (1991).
[33] D. R. McKenzie, W. D. McFall, W. G. Sainty, C. A. Davis, and R. E. Collins, Diamond Relat. Mater. **2**, 970 (1993).
[34] B. Diu, C. Guthmann, D. Lederer, and B. Roulet, *Grundlagen der Statistischen Physik* (de Gruyter, Berlin, 1994), pp. 96-106.
[35] S. J. Chey, L. Huang, and J. H. Weaver, Phys. Rev. B **59**, 16 033 (1999).
[36] B. J. Winter, E. K. Parks, and S. J. Riley, J. Chem. Phys. **94**, 8618 (1991).
[37] R. Fournier, J. Chem. Phys. **115**, 2165 (2001).
[38] W. A. Saunders, Phys. Rev. Lett. **64**, 3046 (1990).
[39] A. Königer, C. Hammerl, M. Zeitler, and B. Rauschenbach, Phys. Rev. B **55**, 8143 (1997).
[40] H. Brune, Surf. Sci. Rep. **31**, 121 (1998).
[41] W. Möller, W. Eckstein, and J. P. Biersack, Comput. Phys. Commun. **51**, 355 (1988).
[42] W. Eckstein, *Computer Simulation of Ion-Solid Interaction* (Springer, Berlin, 1991).